

23. Chen, L. F., Qiu, S. H. and Peng, Z. H., Effects of sanguasaponin on blood lipids and subgroups of high density lipoprotein cholesterol in hyper lipoidemia rat models. *Pharm. Clin. Chin. Mater. Med.*, 1998, **14**, 13–16.
24. Ravichandran, R. and Dhandapani, M., Composition characteristics and potential uses of South Indian tea seeds. *J. Food Sci. Technol.*, 1992, **29**, 394–396.
25. Rajaei, A., Barzegar, M. and Yamini, Y., Supercritical fluid extraction of tea seed oil and its comparison with solvent extraction. *Eur. Food Res. Technol.*, 2005, **220**, 401–405.
26. Sengupta, C., Sengupta, A. and Ghosh, A., Triglyceride composition of tea seed oil. *J. Sci. Food Agric.*, 1976, **27**, 1115–1122.
27. Tokue, C., Kataoka, E. and Tanimura, W., Characterization of lipids in tea (*Camellia sinensis*) seeds cultivated in Taiwan and Japan. *J. Jpn. Soc. Nutr. Food Sci. (Jpn)*, 1989, **42**, 71–77.
28. Ravichandran, R., Fat stability and amino acids in south Indian tea seeds. *Int. J. Food Sci. Technol.*, 1993, **28**, 639–646.
29. Deng, P. J., Zhang, Y. H. and Huang, J. X., A study of the effect of tea seed oil on serum lipid in normal adults. *Acta Nutrimenta. Sinica.*, 1993, **15**, 289–292.
30. Ataii, D., Sahari, M. A. and Hamedi, M., Some physico-chemical characteristics of tea seed oil. *J. Sci. Technol. Agric. Nat. Resour.*, 2003, **7**, 173–183.
31. Hua, G., Jianping, Z., Junwu, L., Huiyuan, T. and Dongmin, L., Fatty acid composition analysis of tea seeds oil. *China Oils Fats*, 2008, **7**.
32. Kiritsakis, A. K., Virgin oil composition and its effect of human health. *Info.*, 2002, **13**, 237–241.
33. Moreau, R. A., Corn oil. In *Composition, Properties, and Uses* (ed. Gunstone, F. D.), Vegetable Oils in Food Technology, Osney Mead, Oxford, Blackwell, CRC Press, Boca Raton, 2002, pp. 282–284.

ACKNOWLEDGEMENT. K.S. acknowledges the financial help in the form of DST Inspire Fellowship to carry out this study.

Received 7 December 2017; accepted 2 March 2018

doi: 10.18520/cs/v114/i12/2549-2554

## Incessant erosion of high tidal mudflats in the northern Gulf of Khambhat

Hiren Bhatti\*, Ratheesh Ramakrishnan, A. K. Sharma and A. S. Rajawat

Space Applications Centre, Jodhpur Tekra, Ahmedabad 380 015, India

**Extensive erosion of high tidal mudflat along the northern parts of Gulf of Khambhat (GoK) was observed from the analysis of time series satellite images during the time period from March 2014 to September 2017. Around 28.66 sq. km area of high tidal mudflat eroded within this time period. Maxi-**

**imum erosion rates estimated have even peaked to about 4 km/year showing the severity of erosion. The mudflats under erosion are along the outer boundary of a meandering tidal channel connecting the Gulf with Mahi river. A possible cause of the incessant erosion of mudflats is the strong tidal currents along the outer boundary of the meandering tidal channel, that have carved the mudflats and pushed the tidal channel further landward. A subtle seasonal pattern of erosion was observed with decrease in erosion rates during the summer monsoon period when the high tidal currents are weak due to the river influx. Rapid erosion of the tidal mudflats has not only destroyed the vital habitat, but has also eventually exposed the inhabited land area to tidal flooding, making it vulnerable to erosion. The study shows the importance of assessing the stability of mudflats along the GoK, where large development activities are proposed.**

**Keywords:** DSAS, erosion, high tidal mudflat, satellite data, tidal channel.

EROSION of the coastal region poses a major threat not only to the human population, but also to the vital coastal ecosystem. The dynamic interaction between nearshore features and the hydrodynamics of the region, termed as coastal processes, determines the stability of the adjacent shoreline. Moreover, various developments along the coast enhance the changes in the shoreline. Coastal erosion is considered as a major threat worldwide and India, consisting of a long shoreline on the either side of its peninsular is also subjected to erosion in varied strengths<sup>1</sup>.

Satellite data has proved its applicability in deciphering various coastal processes by providing synoptic observations with high temporal coverage. Monitoring shoreline changes is essential in understanding the various coastal processes, developmental planning and estimating regional scale sediment erosion and accretion<sup>2,3</sup>.

The present study involves monitoring the erosion of high tidal mudflat along the Gulf of Khambhat (GoK) using sequential satellite images. Only limited studies carried out based on satellite observations comprehend the coastal dynamics of GoK<sup>4-6</sup>. GoK is a tidal regime located along the west coast of India, which is a north-south penetration of the Arabian Sea between Saurashtra and the Indian Peninsula (Figure 1). The tide range within the gulf reaches about 10 m at Bhavnagar<sup>7</sup>, which is the largest along the Indian coast.

The coastal geomorphology of the gulf is predominantly of tidal mudflats, occupying an area of about 2588 sq. km (refs 8, 9). Although the gulf is a tide dominated region, five major rivers forming an estuary along the coast of Khambhat contribute significantly to its hydrodynamics.

Coastal erosion along the northern part of GoK was monitored using temporal satellite images for a period of 3.5 years. Cloud free Landsat 8 Operational Linear

\*For correspondence. (e-mail: hmbhatti777@gmail.com)

Infrared (OLI) images from March 2014 to September 2017 were downloaded from the USGS site<sup>10</sup>. The list of satellite data along with the corresponding tidal height at Bhavnagar is given in Table 1.

Due to its elevated terrain, the high tidal mudflat along the study region is seldom inundated even during high tide conditions. The geomorphology of the region was clearly distinguished from the intertidal zone due to its

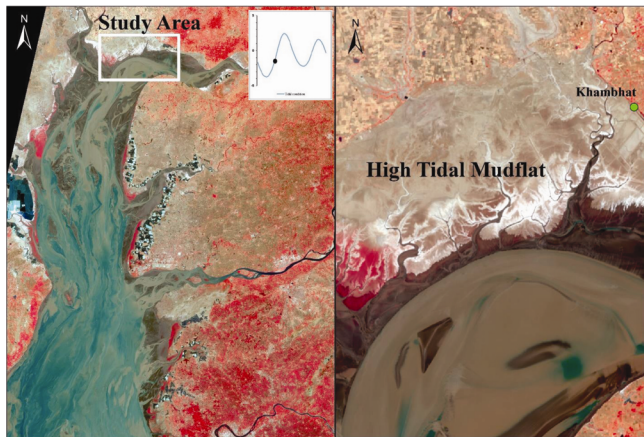


**Figure 1.** The study area composed of northern part of Gulf of Khambhat with high tidal mudflat.

**Table 1.** Tidal height during scenes acquisition

Date	Tidal height
27 March 2014	5.52
14 May 2014	1.13
17 July 2014	5.18
19 September 2014	5.87
5 October 2014	5.82
6 November 2014	2.39
8 December 2014	3.17
24 December 2014	3.04
9 January 2015	4.55
10 February 2015	5.63
1 May 2015	3.05
10 June 2015	8.03
6 September 2015	8.47
8 October 2015	5.69
9 November 2015	3.71
11 December 2015	3.03
12 January 2016	3.12
29 February 2016	5.61
16 March 2016	7.68
17 April 2016	5.09
19 May 2016	2.63
4 June 2016	0.9
26 October 2016	5.74
27 November 2016	3.65
29 December 2016	3.17
3 March 2017	4.59
22 May 2017	5.52
27 September 2017	6.74

difference in moisture. Visual interpretation of the high tidal mudflat was carried out using infrared colour composite images, where the tonal contrast between the dry and moist sediments due to absorption of water at the infrared channel was enhanced to demarcate the boundary distinctly.

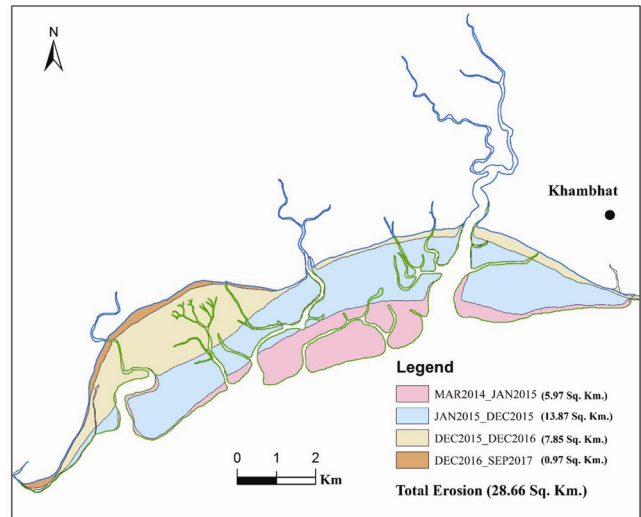


**Figure 2.** Erosion of mudflats along the northern parts of the Gulf of Khambhat.

**Table 2.** LANDSAT-8 (OLI) scenes used and summary of the erosion rates computed using digital shoreline analysis system

Period	Average erosion rate (m/year)	Maximum erosion rate (m/year)
27 March–14 May 2014	180.81	387.46
14 May–17 July 2014	515.9	2384.29
17 July–19 September 2014	1026.53	2026.52
19 September–5 October 2014	150.37	398.78
5 October–6 November 2014	1957.64	3504.61
6 November–8 December 2014	1777.89	3911.06
8 December–24 December 2014	1678.28	4071.31
24 December 2014–9 January 2015	1981.86	3934.69
9 January–10 February 2015	1538.72	3494.68
10 February–1 May 2015	1115.24	2293.64
1 May–10 June 2015	1610.88	3231.94
10 June–6 September 2015	1179.72	1819.57
6 September–8 October 2015	731.79	1840.02
8 October–9 November 2015	796.27	2826.06
9 November–11 December 2015	653.49	2202.18
11 December 2015–12 January 2016	1084.54	3074.9
12 January–29 February 2016	1390.4	3408.17
29 February–16 March 2016	1159.8	3668.86
16 March–17 April 2016	1183.69	2072.29
17 April–19 May 2016	1456.12	4203.25
19 May–4 June 2016	950.69	2134.16
4 June–26 October 2016	364.34	1424.7
26 October–27 November 2016	498.16	1322.63
27 November–29 December 2016	628.61	1289.76
29 December 2016–3 March 2017	171.7	679.29
3 March–22 May 2017	164.85	509.01
22 May–27 September 2017	110.77	300.07
Total	965.15	

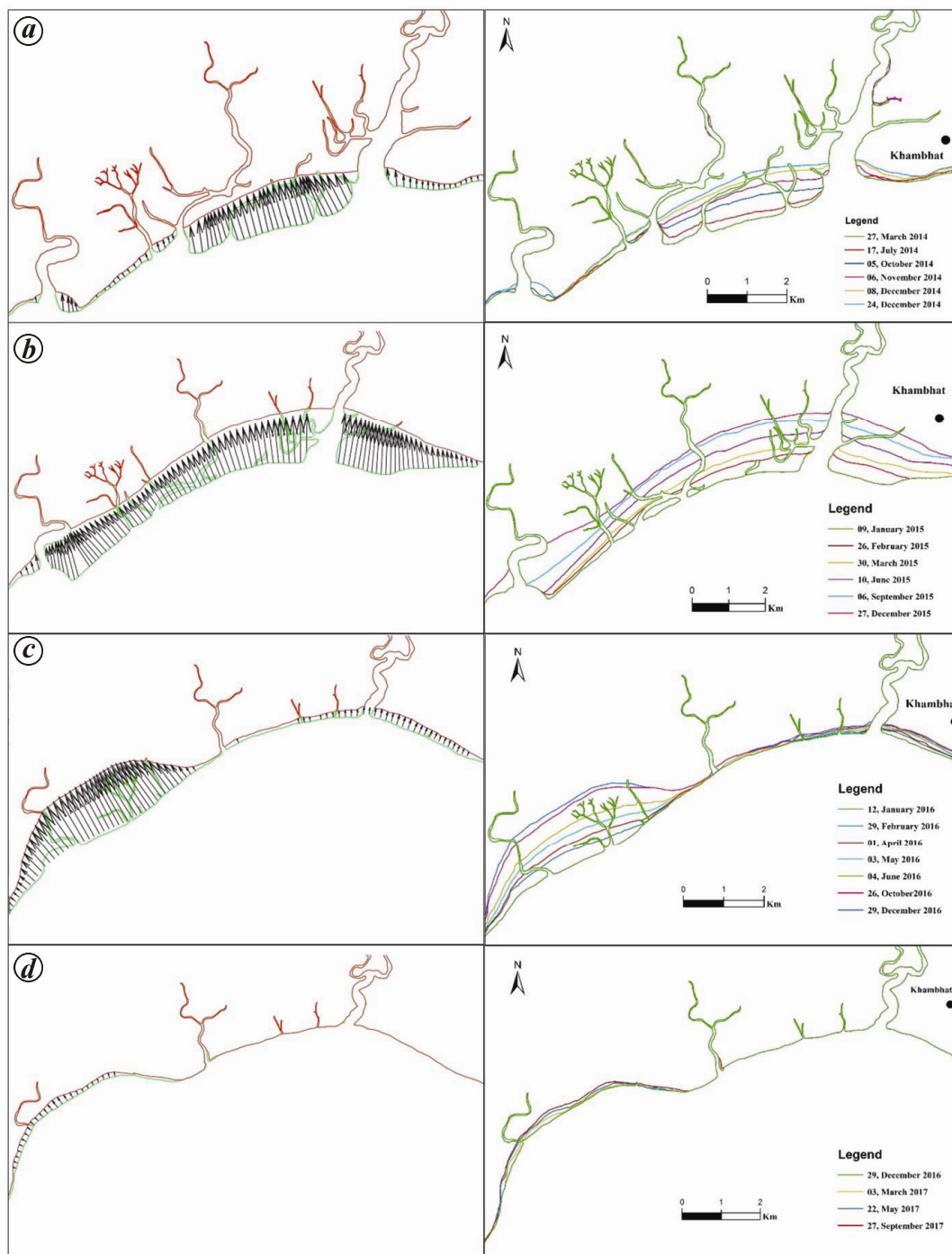


**Figure 3.** Erosion rates estimated during the years (a) 2014, (b) 2015, (c) 2016 and (d) 2017.

Erosion rate of the mudflats was computed using Digital Shoreline Analysis System (DSAS). End point rate (EPR) was used to estimate the erosion rates. The eroding mudflat at GoK was about 20 km in length and erosion rates were calculated for each segment separated by a distance of 50 m.

The seaward boundary of the high tidal mudflat was mapped for each satellite data. From the analysis, high

tidal mudflats of the northern GoK were observed to be severely eroded. Area of the high tidal mudflat that eroded from March 2014 to September 2017 is shown in Figure 2. The total erosion of the high tidal mudflat was observed to be around 28.66 sq. km. The temporal sequence of the erosion pattern is also depicted in Figure 2. In 2014, a total of 5.97 sq. km of mudflat area was observed to be eroded. During 2015 the erosion peaked

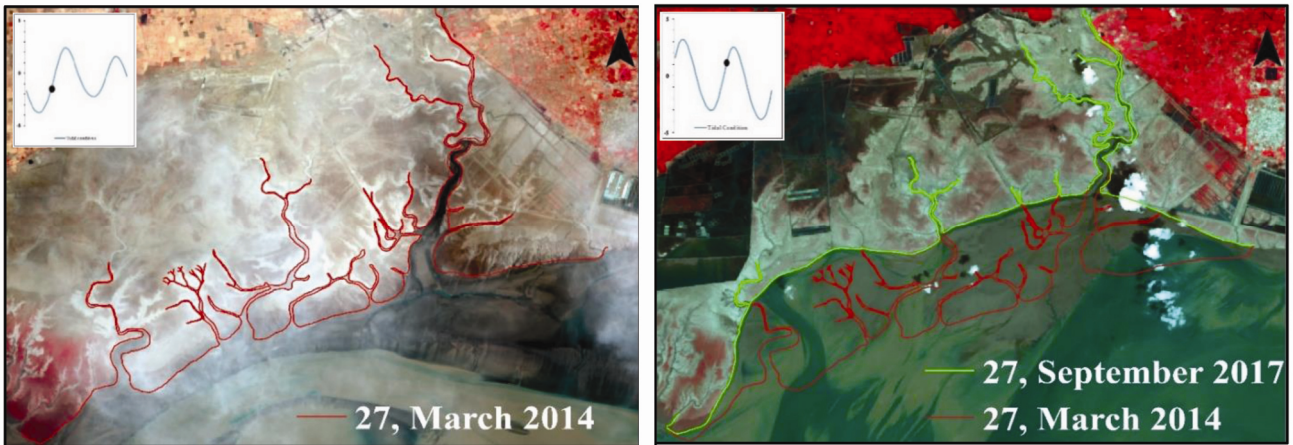


**Figure 4.** Erosion of tidal mudflats as observed from LANDSAT images of April 2014 and September 2017.

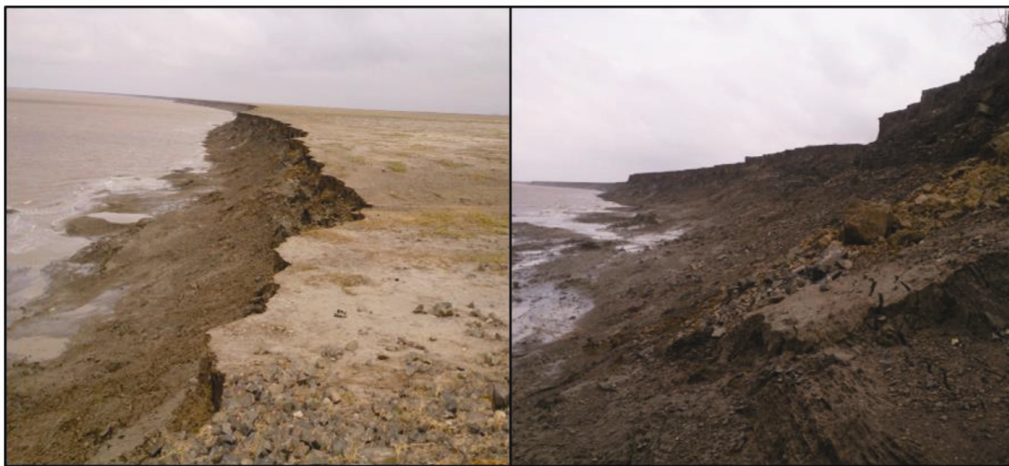


**Figure 5.** Field photograph of high tidal mudflat in northern Gulf of Khambhat.

and caused a loss of around 13.87 sq. km of high tidal mudflats. Erosion of high tidal mudflats for 2016 was about 7.85 sq. km and subsequently during 2017 (until September 2017) around 1 sq. km of high tidal mudflats were eroded.

Erosion rates calculated using DSAS between consecutive satellite images are given in Table 2. The average erosion along the mudflat peaked during the winter months of 2014 and pre-monsoon months of 2015. Maximum erosion rate computed was about 3.5–4 km/year, which implies that at certain locations, about 10 m of land eroded each day.

Even though a clear seasonal pattern was not observed, the maximum and average erosion rates were more during the winter monsoon and pre-monsoon seasons when compared to the summer monsoon season. The possible reason may be due to increased volume of fresh water in the gulf especially along the Mahi and Sabarmati river mouths, which prevented the strengthening of current velocity during the high tide.

The estimated erosion rates were used to prepare vector plots to decipher the sequence in the eroding trends. Figure 3 shows the erosion rate between two selected consecutive images. Magnitude of the vector depicts the erosion rate and direction is the azimuth of transects created by DSAS for computation of the erosion rate.

The erosion rate and its vector estimated for the high tidal mudflats between March 2014 and December 2014 are shown in Figure 3 *a*. The erosion was along the central region of the tidal mudflat, while the mudflats to the east and west were observed to have small scale changes. During 2015 (Figure 3 *b*), the erosion rate was at its peak, covering the entire mudflat.

The erosion rate during 2016 depicted in Figure 3 *c*, shows the enhanced erosion of high tidal mudflats along the western parts of the study region. Erosion rates peaked during the pre-monsoon period to about 3.5 km/year. The erosion rate (Figure 3 *d*) significantly reduced during 2017 and was only along the western parts of the study region.

The erosion of high tidal mudflats along GoK was observed to be confined along the northern periphery of the tidal channel linking the gulf with Mahi River. The tidal channels along this region made meanders and the outer banks of the meandering tidal channel have strong current velocities with a potential to erode the coast along its outer periphery. These strong tidal currents along the outer periphery of meanders had possibly initiated the erosion by carving the high tidal mudflats and further causing the tidal channels to migrate landwards.

The massive erosion resulted in extensive changes of the geomorphology along the study region (Figure 4). Figure 5 shows the field photo of the eroded mudflat at northern GoK. The erosion created a vertical scrap of around 10 m showing the severity of the erosion.

Even though the high tidal mudflat is uninhabited, extensive erosion has led to the destruction of a large area of vital habitat. The western parts of the mudflat that were eroded during 2016, nurtured the growth of mangrove. Due to the erosion, coastal settlements near the mudflats are prone to erosion or flooding during high tide condition. Conventional coastal protection measures like seawall or groins are not recommended along the mudflat region due to its soft bottom sediments. To arrest erosion, novel approaches that can reduce the current velocity along the outer channels should be adopted by the coastal management authority.

Another major outcome of erosion is the change in regional hydrodynamics owing to the deposition of the huge volume of eroded materials elsewhere. As the study region is subjected to anthropogenic pressure and is a hotspot for major development activities, a proper study on the further stability of the mudflats, the extent of the impact of erosion, changes in the hydrodynamics of the region are essential requirements for sustainable development.

1. Rajawat, A. S. *et al.*, Assessment of coastal erosion along the Indian coast on 1 : 25,000 scale using satellite data of 1989–1991 and 2004–2006 time frames. *Curr. Sci.*, 2015, **109**(2), 347–353.
2. Sherman, D. J. and Bauer, B. O., Coastal geomorphology through the looking glass. *Geomorphol. Res. Frontier Beyond*, 1993, **7**, 225–249.
3. Zuzek, P. J., Robert, B. N. and Scott, J. T., Spatial and temporal considerations for calculating shoreline change rates in Great Lakes Basin. *J. Coast. Res.*, 2003, **38**, 125–146.
4. Kunte, P. D., Sediment concentration and bed form structures of Gulf of Cambay from remote sensing. *Int. J. Remote Sensing*, 2008, **29**(8), 2169–2182.
5. Misra, A. R., Murli, M., Sukumaran, S. and Vethamony, P., Seasonal variation of total suspended matter (TSM) in the gulf of Khambhat, west coast of India. *Indian J. Mar. Sci.*, 2014, **43**(7), 1202–1209.
6. Gupta, M., Monitoring shoreline changes in the Gulf of Khambhat, India during 1966–2004 using Resourcesat-1 LISS-III. *Open J. Remote Sensing Position*, 2014, **1**(1), 27–37.
7. Unnikrishnan, A. S., Shetye, S. R. and Michael, G. S., Tidal propagation in the Gulf of Khambhat, Bombay high, and surrounding

areas. *Proc. Indian Acad. Sci., Earth Planet. Sci.*, 1999, **108**, 155–177.

8. Nayak, S. R. and Sahai, B., Coastal morphology: a case study of the gulf of Khambhat (Cambay). *Int. J. Remote Sensing*, 1985, **6**, 559–567.
9. ICMAM (Integrated Coastal and Marine Area Management) Project Directorate; Chennai. Geographical Information System for Gulf of Kutch, Department of Ocean Development, Government of India, 2002.
10. <http://earthexplorer.usgs.gov>

ACKNOWLEDGEMENTS. We thank Shri Tapan Mishra, Director, SAC, Ahmedabad for providing guidance and support. We also thank Dr Rajkumar, Deputy Director, EPSA, SAC, Ahmedabad for providing valuable guidance and constant encouragement.

Received 15 January 2018; revised accepted 6 March 2018

doi: 10.18520/cs/v114/i12/2554-2558

## Effect of synthetic astaxanthin, Lucantin on colour and physical quality of Indian white prawn, *Fenneropenaeus indicus*

Sambhu Chithambaran<sup>1,\*</sup> and Nasser K. Ayaril<sup>2</sup>

<sup>1</sup>Department of Marine Biology, Faculty of Marine Sciences, King Abdulaziz University, Jeddah 21589, Saudi Arabia

<sup>2</sup>National Aquaculture Group, Al Lith 21961, Saudi Arabia

**The effect of a synthetic source of astaxanthin, Lucantin on colour, loose shell/soft shell quality, taste and black spot formation of Indian white shrimp, *Fenneropenaeus indicus*, was studied. Supplementary feed incorporated with Lucantin red and pink at 250 ppm was fed for a period of 45 days prior to harvest. Shrimp fed with the normal feed were considered as control. Shrimp colour and quality were assessed after 15, 30 and 45 days of Lucantin feeding. Significant difference in colour was noticed between control and treatment, whereas no significant difference was observed in loose shell/soft shell and black spot formation. Lucantin is found to be a safe feed additive to improve colour in *F. indicus*.**

**Keywords:** *Fenneropenaeus indicus*, Lucantin, shrimp quality, supplementary feed.

AQUACULTURISTS, shrimp processors and importers consider that visual appearance, especially colour, is one of the most important characteristics of shrimp in determining their selection prior to consumption<sup>1</sup>. Colour can

\*For correspondence. (e-mail: sambhu@kau.edu.sa)